Possible constraints on anatectic melt residence times from accessory mineral dissolution rates: an example from Himalayan leucogranites

MICHAEL AYRES, NIGEL HARRIS

Department of Earth Sciences, The Open University, Milton Keynes MK7 6AA, UK

AND

DEREK VANCE

Institut für Isotopengeologie, ETH-Zentrum, 8092 Zürich, Switzerland

Abstract

The concentrations of *LREE* and Zr in a granitic melt formed by anatexis of a metapelitic protolith will be buffered by the stability of monazite and zircon respectively. The rate at which equilibrium is reached between dissolving monazite and zircon and a static melt is limited by the rate at which Zr and *LREE* can diffuse away from dissolution sites. If melt extraction rates exceed the rates at which the *LREE* and Zr in the melt become homogenized by diffusion, extracted melts will be undersaturated with respect to these elements. Evidence from accessory phase thermometry suggests that for many Himalayan leucogranites generated by crustal anatexis, the melts equilibrated with restitic monazite and zircon prior to extraction. In contrast, discordant temperatures determined from accessory phase thermometry suggest that tourmaline leucogranites from the Zanskar region of NW India did not equilibrate prior to extraction. Quantitative interpretation of this discordance assumes that the melt was static prior to extraction, and that accessory phase inheritance was minimal. Modelling of the time-dependant homogenization process suggests that tourmaline leucogranites generated at 700°C probably remained in contact with restitic monazite in the protolith for less than 7 ka and certainly less than 50 ka. Such rapid extraction rates suggest that deformation-driven mechanisms were important in removing these melts from their source.

KEYWORDS: anatexis, melt residence time, leucogranites, Himalayas.

Introduction

A knowledge of the time period during which anatectic melts and their protoliths remain in contact (the melt residence time) is required to further our understanding of the processes which control the chemistry and extraction of crustal melts. In general, conventional radiometric dating techniques poorly constrain melt residence times, since intracrystalline element diffusion usually resets mineral isotope systematics at temperatures below the solidus of metapelitic protoliths.

In this study we use two accessory phase thermometers (Watson and Harrison, 1983; Montel, 1993) to estimate temperatures of anatexis for Miocene Himalayan leucogranites from the Zanskar region of northwest India. Discordance between the thermometers is interpreted as evidence for melt/accessory phase disequilibrium at the time of melt extraction from the protolith, due to differential accessory phase dissolution rates. Experimental diffusion data, which relate to accessory mineral dissolution rates, are used to estimate melt residence times for these granites.

Accessory phase thermometry

The light rare earth elements (*LREE*) and zirconium (Zr) are essential structural components (ESCs) in the accessory phases monazite and zircon respectively.

Mineralogical Magazine, Vol. 61, February 1997, pp. 29–36

During anatexis, melt ESC concentrations are controlled by accessory phase dissolution. Under equilibrium conditions accessory phase dissolution will proceed until ESC saturation in the melt is attained. Subsequently, during cooling of the saturated melt, ESC concentrations will overstep saturation levels and accessory phase crystallization will ensue. Empirical algorithms have been derived from accessory phase dissolution experiments. These relate the concentrations of Zr (Watson and Harrison, 1983) and the *LREE* (Rapp and Watson, 1986; Montel, 1993) in a melt to its temperature, major element composition and water content, where it is assumed that the melt's Zr and *LREE* concentrations are buffered by zircon and monazite stability respectively. Consequently, the concentrations of these elements in a granite can be used as geothermometers. This technique estimates the temperature at which the melt last equilibrated with an accessory mineral, which represents one of the following situations:

(i) The temperature of extraction of a granitic magma from its source, provided that no fractional crystallization has occurred after extraction.

(ii) The temperature of differentiation from a parental magma where fractional crystallization has occurred.

This approach implicitly assumes that: (i) the melt equilibrated with restitic accessory phases; (ii) the melt contains no entrained accessory phases and (iii) sufficient quantities of accessory phase were present in the protolith in order to saturate the melt. If the melt were to contain significant quantities of inherited zircon or monazite, the Zr and *LREE* concentrations would exceed saturation levels, resulting in an overestimation of the magmatic temperature. Alternatively, if the melt had not equilibrated with restitic accessory phases prior to extraction, it would be undersaturated with respect to Zr and/or *LREE* depending on the relative homogenization rates of these elements in the melt (Watt and Harley, 1993). In this case the temperature calculated would be a minimum estimate.

Homogenization of the *LREE* and Zr in a granitic magma

Anatectic melts may result from biotite breakdown, involving a strongly divariant reaction, or from muscovite breakdown, by an incongruent univariant reaction (Harris *et al.*, 1995). Due to the univariant nature of the muscovite breakdown reaction melting is likely to be rapid and will continue until one of the reactant phases is exhausted, and there will be limited opportunity for fractional melting. Assuming that melts formed by incongruent muscovite breakdown are initially static, interstitial and homogeneously distributed, then the time (t) required for diffusional homogenization of an ESC in the melt is given by the approximation:

$$x^2 = D(T)t \quad (1)$$

where $D(T)$ is the temperature-dependent ESC diffusion rate in the melt, and x is the diffusion length-scale. We take x to be half the mean distance between accessory phase grains of the same species. This assumes that the melt, whilst resident within the protolith, is composed of contiguous spheres of radius x, each containing an accessory grain at its centre. Although equation (1) actually describes diffusion in a semi-infinite medium, it produces results which approximate (to within 30%) those obtained using the more rigorous equations describing diffusion within a sphere (Harrison and Watson, 1983). This uncertainty does not warrant a detailed mathematical approach, since, as will be discussed later, it is insignificant in comparison with the uncertainties in ESC diffusion data.

Application of equation (1) assumes that the melt is static; for a dynamic melt x is not defined. In the absence of a driving force (e.g. deformation) melt segregation will proceed slowly (Clemens and Mawer, 1992) and the melt will remain in contact with restitic accessory phases. If the terrain is subsequently deformed and melt segregation and extraction is rapid (e.g. Clemens and Mawer, 1992), the melt will be unable to exchange significantly with restitic or wall-bound accessory phases and its ESC signature at the time of segregation will be preserved. However, if melt segregation commences immediately following the onset of anatexis the melt may flow past wall- or phase-bound accessories at, or below, saturation levels resulting in modification of its Zr and *LREE* contents. Thus, x would not be defined and the use of equation (1) would be inappropriate. Our analysis of magma residence times assumes that melt extraction was a rapid process following the coexistence of a static melt and restite.

Himalayan leucogranites

For realistic calculations of melt residence times the granite must represent a primary unmodified melt. Miocene peraluminous leucogranites intruded into the upper levels of the High Himalayan Crystalline Series (HHCS; Fig. 1) satisfy this criterion; they are interpreted as crustal melts with trace element compositions that are unmodified by post-extraction differentiation or country rock assimilation processes (Deniel *et al.*, 1987; Inger and Harris, 1993). Moreover they have not undergone convective circulation during melt formation (Deniel *et al.*, 1987).

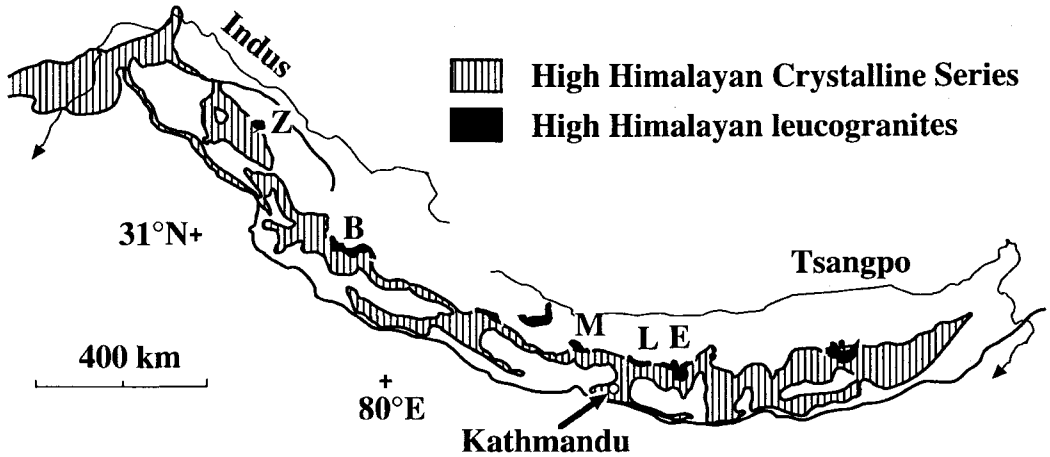

FIG. 1. Geological sketch map of the Himalayas. Miocene leucogranites discussed in text are indicated by Z, Zanskar; B, Badrinath-Gangotri; L, Langtang; E, Everest; M, Manaslu. Modified after Scaillet *et al.* (1990).

Isotopic studies from several Himalayan leucogranites indicate a melting/emplacement age of around 20 Ma (Deniel *et al.*, 1987; Copeland *et al.*, 1990; Ferrara *et al.*, 1991). The protoliths of the Himalayan leucogranites are constrained on the basis of Sr and Nd isotope characteristics to be the metapelitic schists and migmatites within the HHCS (Deniel *et al.*, 1987; France-Lanord and Le Fort, 1988; Harris and Massey, 1994). Modelled melt reactions derived from geochemical and modal analyses of both leucogranites and metapelites indicate that the melts were generated by the incongruent breakdown of muscovite under vapour-absent conditions (Harris *et al.*, 1995; Inger and Harris, 1993).

Two distinct facies of Himalayan leucogranite have been identified; (i) biotite granites, with the assemblage biotite + muscovite + plagioclase + alkali feldspar + quartz ± tourmaline ± garnet, and characterised by low Rb/Sr, and high TiO_2, Ba, *LREE* and La/Lu; (ii) tourmaline leucogranites, with the assemblage tourmaline + muscovite + plagioclase + alkali feldspar + quartz ± biotite, and characterized by high Rb/Sr, and low TiO_2, Ba, *LREE* and La/Lu (Table 1). A recent study of the Manaslu leucogranite from Central Nepal has established that the tourmaline leucogranites are characterized by $(^{87}Sr/^{86}Sr)_0 > 0.752$, $\varepsilon Nd > -15$, whilst biotite leucogranites have $(^{87}Sr/^{86}Sr)_0 < 0.752$, $\varepsilon Nd < -15$, suggesting derivation from distinct protoliths (Guillot and Le Fort, 1995).

The amount of water dissolved in a melt is dependent upon the melting reaction and the pressure at which melting occurs. The maximum water

TABLE 1. Summary of critical geochemical characteristics for Miocene leucogranites from the Zanskar region of the HHCS

	Biotite granites			Tourmaline granites		
	Av	sd	n	Av	sd	n
TiO_2 (wt.%)	0.090	0.036	13	0.057	0.067	26
Rb/Sr	4.0	6.6	13	7.2	6.7	26
Ba (ppm)	223.1	114.7	13	113.2	75.2	26
La/Lu	60.9	11.6	4	41.2	12.8	9
Zr (ppm)	35.7	10.2	13	30.3	8.9	26
*LREE*t	0.39	0.07	4	0.19	0.06	9

Av = Average, sd = Standard deviation, n = number of samples analysed. *LREE*t = $R(X_i/M_i)$, where X is the concentration in ppm of element i, M is the atomic weight of element i, and i is the elements La, Ce, Pr, Nd, Sm and Gd.

content of a eutectic melt in the haplogranite system Qz-Ab-Or-H_2O at 5 kbar is 10 wt.% (Holtz and Johannes, 1995; Clemens, 1984). For leucogranite melts generated by the incongruent breakdown of muscovite, this phase is likely to be the only source of water or hydroxyl ions. Such melts will contain around 6 wt.% H_2O depending on the modal abundance of muscovite in the protolith (Clemens and Vielzeuf, 1987). Scaillet *et al.* (1995) compared the crystallization sequence observed in Himalayan leucogranites with that observed in experimental leucogranite crystallization run products, and concluded that biotite leucogranites had initial water contents of 5–7.5 wt.%, whereas tourmaline leucogranites had initial water contents of >7 wt.%. This is consistent with the experimental results of Pichavant (1987), which demonstrate that high melt B concentrations, as indicated by the presence of tourmaline in the leucogranites, increase melt water solubility. In the following calculations we assume that the melt from which the biotite leucogranites crystallised contained 6 wt.% H_2O, compared with 8 wt.% H_2O for the tourmaline leucogranite melt.

Temperatures of anatexis have been calculated using Zr (Watson and Harrison, 1983) and *LREE* (Montel, 1993) thermometry for samples from three Himalayan leucogranite localities (Fig. 2). Temperatures derived from the biotite leucogranites (700–750°C) are consistently higher than those for the tourmaline leucogranites (660–700°C) from each region. These temperatures are consistent with experimental evidence (Scaillet *et al.*, 1995), and with results of geochemical modelling of leucogranite Rb and Sr concentrations (Inger and Harris, 1993). For the majority of biotite leucogranites there is remarkable agreement between the two thermometers; temperatures differ by less than 10°C. In contrast there is appreciable discordance between *T*(Zr) and *T*(*LREE*) for the tourmaline leucogranites from Zanskar and the biotite leucogranite from Everest. Copeland *et al.* (1988) detected inherited radiogenic Pb in zircon and monazite from the Everest leucogranite, and concluded that a proportion of each accessory mineral was inherited from the protolith. Therefore, for the Everest leucogranite preferential entrainment of monazite may have resulted in a temperature overestimate from monazite thermometry. For the tourmaline granites from Zanskar, *T*(Zr) is consistently higher than *T*(*LREE*). This feature was also noted by Scaillet *et al.* (1990) for the Badrinath granite, although it is not apparent from their published summary dataset. Several mechanisms could be responsible for this observed discordance;

(i) Selective inheritance of accessories. There is no *a priori* method of determining whether monazite or zircon will be preferentially inherited by a melt, since

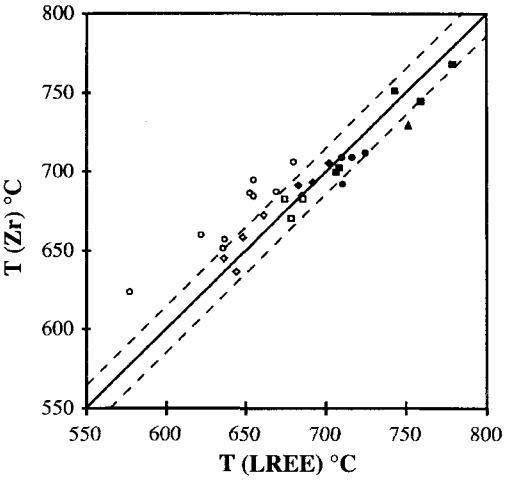

FIG. 2. Plot of *T*(Zr) against *T*(*LREE*), the temperatures calculated by zircon and monazite accessory phase thermometry respectively, assuming 6 wt.% H_2O in the biotite leucogranites and 8 wt.% H_2O in the tourmaline leucogranites. Leucogranite data; circles, Zanskar (this study, Table 1); squares, Langtang (Inger and Harris, 1993); diamonds, Badrinath (Scaillet *et al.*, 1990); triangle, Everest (Copeland *et al.*, 1988). Solid symbols — biotite leucogranites; open symbols — tourmaline leucogranites. Solid line — locus of *T*(Zr) = *T*(*LREE*); dashed lines enclose data within 10°C of concordance.

there is little density contrast between these phases, and they are of similar grain size in Himalayan metapelitic protoliths. However, inheritance is likely to be a random process resulting in wide variations in leucogranite trace element chemistry and inferred temperatures within individual granite facies. The Himalayan data (Fig. 2) suggest that inheritance did not play a significant role in determining leucogranite trace element abundances.

(ii) Paucity of accessory phases in the protolith. If the leucogranite protoliths (e.g. metapelites in the HHCS) contained insufficient quantities of either zircon or monazite to saturate a melt in Zr or the *LREE* respectively, then anomalously low melt temperatures would be obtained from one or both of the accessory phase thermometers. This might mistakenly be interpreted as evidence for melt/accessory phase disequilibrium during anatexis. Thus, it is necessary to determine whether HHCS metapelites contain sufficient zircon and monazite in order to saturate a melt in Zr and the *LREE*. For a melt of similar bulk composition to the Himalayan biotite leucogranites containing 6 wt.% H_2O at 750°C, Zr and Ce saturation levels are 88 ppm and 38 ppm respectively. Muscovite dehydration melting

of a pelitic protolith is not thought to generate melt fractions larger than 0.2 (Harris *et al.*, 1995; Clemens and Vielzeuf, 1987). Therefore, in order for a melt to obtain these trace element concentrations, the protolith is required to contain >17.6 ppm Zr and >7.6 ppm Ce. The Zr and Ce concentrations of HHCS metapelites from Zanskar are considerably higher (average 200 ppm and 82 ppm respectively). However, a proportion of each accessory phase will be occluded within restitic phases and therefore shielded from the melt during anatexis. In a study of the distribution of accessory phase grains in a migmatite from the Tibetan Slab (HHCS), Watson *et al.* (1989) calculated that approximately 70% of the accessory phase grain population occurred as inclusions within major phases. However, since included accessory grains tended to be smaller than those sited at grain-boundaries, 70% of the accessory phase mass occurred at grain-boundaries. Therefore, even if only 70% of a protolith's total Zr and Ce budgets are available to a melt, it is unlikely that either zircon or monazite would become entirely dissolved during melting.

(iii) Contrasting dissolution kinetics for zircon and monazite. Since zircon dissolves more rapidly than monazite in a granite melt (Harrison and Watson, 1983; Rapp and Watson, 1986), the temperature discordance inferred from monazite and zircon thermometry could result from rapid melt extraction. The systematically low *T(LREE)* values from the Zanskar tourmaline leucogranites may therefore indicate undersaturation of *LREE* in the melt, as a result of melt/restitic monazite disequilibrium at the time of melt extraction. This interpretation is evaluated in the following section.

Himalayan leucogranite residence times

The appropriate diffusion length-scale (x) has to be determined before equation (1) can be applied to calculate ESC homogenization times. We have adopted two approaches to establish values of x for monazite and zircon.

Firstly, the spatial distribution of monazite and zircon grains within a 35 mm^2 area of a typical medium-grained subsolidus kyanite-grade metapelite has been determined using back-scattered electron (BSE) imaging and electron-dispersive spectroscopy. In total, 78 zircon grains and 9 monazite grains were observed. Zircon grains (<30 μm diameter) are, in general, smaller than monazite grains (<50 μm diameter). Host phases of zircon inclusions, in decreasing order of significance, are garnet (29 grains), muscovite (23), bioite (4). The remaining 22 grains were sited at grain boundaries. Grains sited at grain boundaries and those occurring as inclusions within muscovite will be able to dissolve in a melt. For monazite, only three grains were included within biotite or garnet. Although the sample population is small, it is possible to calculate the mean two-dimensional spatial distribution of zircon (x = 0.4 mm) and monazite (x = 1.2 mm) grains available for interaction with a melt, providing maximum constraints on actual three-dimensional diffusion length-scales.

Secondly, since monazite and zircon contain almost the entire respective *LREE* and Zr budgets of a typical metapelite (Harris *et al.*, 1995) normative abundances of these minerals can be calculated from whole-rock trace element data. The three-dimensional distribution of zircon and monazite grains can be estimated if the average radius of each accessory phase is known (and allowing for the proportion of accessories included in biotite and garnet, estimated at 30% by Watson *et al.*, 1989). Average grain sizes have been obtained by BSE examination of monazite and zircon grains in three HHCS metapelites. The calculated diffusion length-scales (x) for monazite and zircon are 0.4 ± 0.16 mm and 0.2 ± 0.08 mm respectively. These values are consistent with the length-scales obtained by direct observation, and are the values adopted in the following calculations. The uncertainty in x is derived primarily from the uncertainty associated with estimating mean accessory phase grain sizes.

For a given length-scale the time required to homogenize either Zr or the *LREE* in a melt is a function of its temperature and water content. Zr diffusion data have been obtained experimentally for melt water contents of <0.2 wt.% and 6 wt.% (Harrison and Watson, 1983). An increase in melt H_2O content from 2 wt.% to 5 wt.% results in a five-fold increase in the rate of Zr diffusion in the melt. However, for melts with less than 2 wt.% H_2O, Zr diffusion rates decrease dramatically (Harrison and Watson, 1983). *LREE* diffusion data have been determined for melts with 1, 2, 4 and 6 wt.% H_2O (Rapp and Watson, 1986). *LREE* diffusion rates in a granitic magma increase monotonically with increasing melt water content (Rapp and Watson, 1986).

Using appropriate melt water contents and diffusion length-scales, comparison of Zr and *LREE* homogenization times over the temperature range 660°C–760°C illustrates that Zr homogenization in a melt is three orders of magnitude faster than *LREE* homogenization (Fig. 3). Monazite dissolution rates are unlikely to be controlled by phosphorous diffusion, since experimental data suggest that phosphorous diffusion rates are up to four orders of magnitude faster than *LREE* diffusion rates (Wolf and London, 1994; Harrison and Watson, 1983, 1984).

For the biotite granites generated at solidus temperatures of 700°C–750°C, homogenization

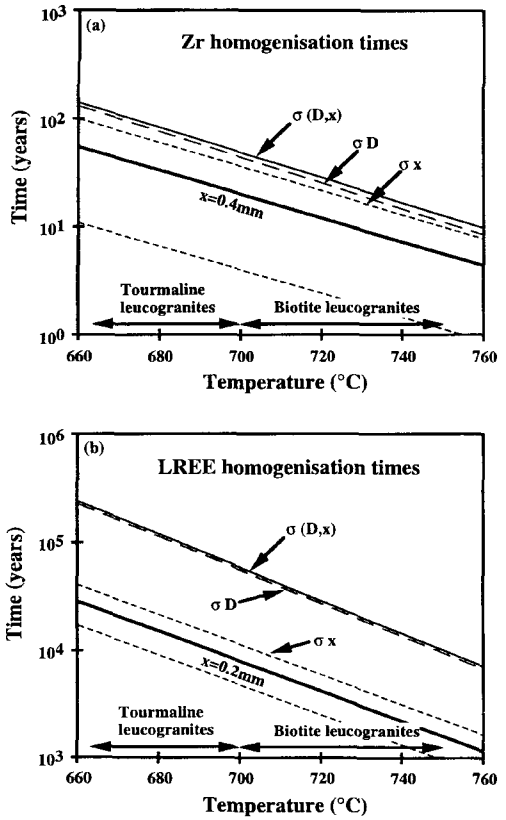

FIG. 3. (*a*) Zr and (*b*) *LREE* homogenization times (ordinate) as a function of diffusion length-scale (*x*, thick solid line), and temperature, calculated using equation (1) assuming 6 wt.% H_2O in the melt. Combined uncertainty ($\sigma_{D,x}$; thin solid line) calculated by propagating the uncertainties in the diffusion length-scale (σ_x; short dashed line) and diffusion data (σ_D; long dashed line). Note that lower error envelopes cannot be illustrated where relative standard deviation is greater than 100%. Diffusion data for Zr from Harrison and Watson (1983), and *LREE* from Rapp and Watson (1986).

times are 18 ± 23 to 6 ± 8 years for Zr, and 7 ± 40 ka to 2 ± 10 ka for the *LREE*. These are minimum melt residence times, since these melts equilibrated with restitic monazite and zircon prior to extraction. The uncertainties, which include those inherent from the diffusion data and from our estimates of diffusion length-scales, are illustrated in Fig. 3. For both Zr and the *LREE*, the magnitude of the total uncertainty in homogenization times is dominated by the uncertainty in the diffusion data. Such large uncertainties mean that no geologically significant information can be obtained on melt residence times where zircon and monazite temperatures are concordant.

For temperatures appropriate to the generation of the tourmaline leucogranites (solidus temperatures of 660–700°C) and for the calculated diffusion length-scales, Zr homogenization takes 50 ± 70 to 18 ± 23 years, whilst *LREE* homogenization takes 30 ± 150 ka to 7 ± 40 ka. The temperatures indicated by accessory phase thermometry for tourmaline granites from Langtang and Badrinath (Fig. 2) are concordant, indicating that the calculated melt residence times are minimum constraints. However, $T(\mathrm{Zr}) > T(LREE)$ for tourmaline leucogranites from Zanskar, suggesting that insufficient time was available for these magmas to equilibrate with restitic monazite prior to extraction. Calculated *LREE* homogenization times are therefore maximum constraints for the duration of dissolution prior to melt extraction.

Discussion and conclusions

For the majority of Himalayan leucogranites, where melts reached chemical equilibrium with monazite and zircon in the protolith prior to extraction, calculated constraints for the minimum magma residence times are rendered meaningless by the large uncertainties. However, systematic discordance between temperatures calculated from zircon and monazite thermometry may carry information on melt residence times. For example, if the temperature discordance recorded by the tourmaline leucogranites from Zanskar results from disequilibrium, then it is probable that the melt remained in contact with restitic monazite for less than 50 ka at 700°C, or 180 ka at 660°C.

The conclusion that maximum residence times for some tourmaline leucogranites are less than 180 ka supports the view that sluggish *HREE* intracrystalline diffusion rates in garnet will prevent *HREE* equilibration between melt and restitic garnet during anatexis (Harris *et al.*, 1995). Disequilibrium will result in relatively flat chondrite normalised *REE* profiles for anatectic melts even if the protolith includes garnet. Indeed, for such rapid rates of melt extraction, the overall *REE* budget of the melt will be determined, not by equilibrium exchange with restitic phases, but by the relative dissolution rates of accessory phases in the protolith. Additionally, the apparent brevity of source residence times supports a deformation-driven melt segregation and extraction mechanism (Rutter and Neumann, 1995; Clemens and Mawer, 1992), since gravity driven segregation processes are ineffective over this time period (McKenzie, 1985; Wickham, 1987).

This study demonstrates the potential of a simple technique for constraining melt residence times for

rapidly extracted melts formed under static conditions, provided accessory phase inheritance is insignificant. Its usefulness will be greatly enhanced once more precise Zr and *LREE* diffusion data are obtained over a wide range of magma compositions.

Acknowledgements

We thank John Watson and Peter Webb for help with XRF analyses, Nick Rogers for help with INAA, Joanne Hunt for assistance with the SEM at the Open University and Mike Searle for invaluable support during field work. Fieldwork for MA was supported by a NERC studentship. The authors wish to thank Bill Rogan and Phil Bland for their comments on an earlier version of the manuscript, and Simon Harley and Gordon Watt for their thorough and constructive reviews.

References

Clemens, J.D. (1984) Water contents of silicic to intermediate magmas. *Lithos*, **17**, 273–387.

Clemens, J.D. and Mawer, C.K. (1992) Granitic magma transport by fracture propagation. *Tectonophysics*, **204**, 339–60.

Clemens, J.D. and Vielzeuf, D. (1987) Constraints on melting and magma production in the crust. *Earth Planet. Sci. Lett.*, **86**, 287–306.

Copeland, P., Parrish, R.R. and Harrison, T.M. (1988) Identification of inherited radiogenic Pb in monazite and its implications for U-Pb systematics. *Nature*, **333**, 760–3.

Copeland, P., Harrison, T.M. and Le Fort, P. (1990) Age and cooling history of the Manaslu granite: implications for the Himalayan tectonics. *J. Volcanol. Geotherm. Res.*, **44**, 33–50.

Deniel, C., Vidal, P., Fernandez, A., Le Fort, P. and Peucat, J.-J. (1987) Isotopic study of the Manaslu granite (Himalaya, Nepal): inferences on the age and source of Himalayan leucogranites. *Contrib. Mineral. Petrol.*, **96**, 78–92.

Ferrara, G., Lombardo, B., Tonarini, S. and Turi, B. (1991) Sr, Nd and O isotopic characterization of the Gophu La and Gumburanjun leucogranites (High Himalaya). *Schweiz. Mineral. Petrogr. Mitt.*, **71**, 35–51.

France-Lanord, C. and Le Fort, P. (1988) Crustal melting and granite genesis during the Himalayan collision orogenesis. *Trans. R. Soc. Edin.*, **79**, 183–95.

Guillot, S. and Le Fort, P. (1995) Geochemical constraints on the bimodal origin of High Himalayan leucogranites. *Lithos*, **35**, 221–34.

Harris, N., Ayres, M. and Massey, J. (1995) Geochemistry of granitic melts produced during the incongruent melting of muscovite; Implications for the extraction of Himalayan leucogranite magmas. *J. Geophys. Res.*, **100**, 15767–77.

Harris, N.B.W. and Massey, J.A. (1994) Decompression and anatexis of Himalayan metapelites. *Tectonics*, **13**, 1537–46.

Harrison, T.M. and Watson, E.B. (1983) Kinetics of zircon dissolution and zirconium diffusion in granitic melts of variable water content. *Contrib. Mineral. Petrol.*, **84**, 66–72.

Harrison, T.M. and Watson, E.B. (1984) The behavior of apatite during crustal anatexis: Equilibrium and kinetic considerations. *Geochim. Cosmochim. Acta*, **48**, 1467–77.

Holtz, F. and Johannes, W. (1995) Maximum and minimum water contents of granitic melts: implications for chemical and physical properties of ascending magmas. *Lithos*, **32**, 149–59.

Inger, S. and Harris, N. (1993) Geochemical constraints on leucogranite magmatism in the Langtang Valley, Nepal Himalaya. *J. Petrol.*, **34**, 345–68.

McKenzie, D. (1985) The extraction of magma from the crust and mantle. *Earth Planet. Sci. Lett.*, **74**, 81–91.

Montel, J.-M. (1993) A model for monazite/melt equilibrium and application to the generation of granitic magmas. *Chem. Geol.*, **110**, 127–46.

Pichavant, M. (1987) Effects of B and H_2O on liquidus phase relations in the haplogranite system at 1 kbar. *Amer. Mineral.*, **72**, 1056–70.

Rapp, R.P. and Watson, E.B. (1986) Monazite solubility and dissolution kinetics: implications for the thorium and light rare earth chemistry of felsic magmas. *Contrib. Mineral. Petrol.*, **94**, 304–16.

Rutter, E.H. and Neumann D.H.K. (1995) Experimental deformation of partially molten granites under fluid-absent conditions with implications for extraction of granite melts. *J. Geophys. Res.*, **100**, 15697–715.

Scaillet, B., France-Lanord, C. and Le Fort, P. (1990) Badrinath-Gangotri plutons (Garhwal, India): petrological and geochemical evidence for fractionation processes in a high Himalayan leucogranite. *J. Volcanol. Geotherm. Res.*, **44**, 163–88.

Scaillet, B., Pichavant, M. and Roux, J. (1995) Experimental crystallization of leucogranite magmas. *J. Petrol.*, **36**, 663–705.

Watson, E.B. and Harrison, T.M. (1983) Zircon saturation revisited: temperature and composition effects in a variety of crustal magma types. *Earth Planet. Sci. Lett.*, **64**, 295–304.

Watson, E.B., Vicenzi, E.P. and Rapp, R.P. (1989) Inclusion/host relations involving accessory minerals in high-grade metamorphic and anatectic rocks. *Contrib. Mineral. Petrol.*, **101**, 220–31.

Watt, G.R. and Harley, S.L. (1993) Accessory phase controls on the geochemistry of crustal melts and restites produced during water-undersaturated partial melting. *Contrib. Mineral. Petrol.*, **114**, 550–66.

Wickham, S.M. (1987) The segregation and emplacement of granitic magmas. *J. Geol. Soc. London*, **144**, 281–97.

Wolf, M.B. and London, D. (1994) Apatite dissolution into peraluminous haplogranitic melts: An experimental study of solubilities and mechanics. *Geochim. Cosmochim. Acta*, **58**, 4127–45.

[*Manuscript received 3 November 1995: revised 3 June 1996*]